



# VOLUMETRIC IMAGING OF THE FETAL HEART

## TERMINOLOGY<sup>1</sup>

- Three-dimensional (3D): term used to refer to volume datasets defined by 3 spatial dimensions (x, y, and z planes). Since only spatial information is acquired, these volume datasets are static by nature.
- Four-dimensional (4D): refers to volume datasets containing the 3 spatial dimensions plus the temporal dimension. These volume datasets can be displayed with motion and are extensively used for volumetric imaging of the fetal heart.
- Real-time: this term describes a negligible delay between acquisition and display.
- Rendering: technology that allows three-dimensional objects to be displayed on a two-dimensional (2D) screen.
- STIC: acronym for SpatioTemporal Image Correlation. This technology allows retrospective gating of the spatial volumetric data obtained from a beating fetal heart to the fetal heart rate. The process works by re-shuffling of the 2D frames acquired during a sweep through the fetal heart according to the phase of the cardiac cycle at which they were acquired. The result is a series of volume datasets, each representing a phase of the cardiac cycle, which are then played on the screen as a continuous cine loop.<sup>2</sup>

## TRANSDUCER TECHNOLOGY

Volumetric images of the fetal heart can be obtained using mechanical<sup>3-5</sup> or matrix array transducers.<sup>6-9</sup> Mechanical volumetric transducers generally consist of a convex array mounted on a mechanical wobble. The wobble is electronically steered so that it can sweep through a region of interest in an automated fashion. As a result, a series of 2D images with precise x, y, and z spatial coordinates are obtained. Once the images are acquired, they are assembled into a volume dataset, which is then ready to be displayed on a 2D screen using one of several methods described in greater detail below.

Matrix array transducers are electronic transducers composed of thousands of elements arranged on a 2D matrix. All or a portion of the matrix elements can be fired simultaneously, producing a 3D pyramid of sound that can be visualized either as static 3D or as a dynamic real-time 4D volume. Alternatively, rows of elements can be fired in sequence, simulating the volume dataset acquisition process that occurs with mechanical probes.

Both mechanical volumetric and matrix array transducers are capable of producing dynamic volume datasets of the fetal heart using STIC technology.

## VOLUME ACQUISITION

### 2D IMAGE OPTIMIZATION

- Volume acquisition, regardless of transducer technology, begins with optimal 2D imaging. This step is of utmost importance when scanning the fetal heart. The goal is to have a final volume dataset with

good spatial resolution, optimal contrast, and as high as possible temporal resolution. The following are tips to optimize the 2D image prior to volume acquisition:

- Select the transducer with the highest possible frequency for the scanning conditions, taking into account the position of the placenta and maternal body habitus. Obese patients with anterior placentas likely require the selection of a lower frequency transducer.
- Increase the contrast to emphasize a clear distinction between the endocardium, valvular apparatus, and blood pool. This is usually accomplished by adjusting the dynamic range and gain settings to the scanning conditions.
- Make the scanning sector as narrow as possible to maximize the frame rate. This step is particularly important if the volume datasets are acquired with color or power Doppler, since both will negatively impact the frame rate.
- After resolution, contrast, and frame rate are optimized, apply proper magnification.

## REGION OF INTEREST SELECTION

Place the region of interest (ROI) box around the heart. The dimensions of the box, as seen on the screen, determine the amount of data to be acquired in the x- and y-planes. The key here is to pay attention to the width of the ROI. If the ROI is too wide, the frame rate drops, and the final volume dataset may suffer from low temporal resolution. Again, attention to detail in this step is even more important if the volume acquisition is performed with color or power Doppler. As a rule of thumb, select ROIs that include the heart, chest wall, and spine when acquiring volume datasets with gray scale only. If the acquisition involves color or power Doppler, narrow the ROI to include only the heart and great vessels.

## ACQUISITION ANGLE

The angle of acquisition determines the amount of information to be reconstructed in the z-plane. Acquisition angles vary depending on the manufacturer, and can generally be set between 5 and 45 degrees. A large acquisition angle provides more information; however, one needs to remember that fetuses may move during volume acquisition. The goal is to select the narrowest possible angle to include images from the superior mediastinum to the upper abdomen. The basic rules are “small angle for small fetus” and “large angle for large fetus”. It may take some trial and error before one feels comfortable in adjusting this parameter on the fly.

## ACQUISITION TIME

This parameter determines the number of frames that are acquired and incorporated into the final volume dataset. Ideally, longer acquisition time allows more frames to be acquired. This results in a higher spatial resolution, provided that the fetus does not move or moves little during acquisition. Therefore, if the fetus is in an ideal position and not moving, prefer a longer acquisition time. The reverse applies to fetuses that are actively moving. Depending on the manufacturer, acquisition speed ranges from 5 to 15 seconds.

## VOLUME VISUALIZATION METHODS

Once a high quality volume dataset is acquired, it is time to visualize it on the screen and to be able to manipulate it effectively to extract as much diagnostic information as possible. In the following sections, the most commonly used visualization methods are reviewed.

## MULTIPLANAR DISPLAY

Multipanar display is the most commonly used method to visualize volumetric images, regardless of the imaging modality used for acquisition (e.g., computerized tomography, magnetic resonance imaging, ultrasonography, etc.). The screen is usually split into three panels, representing the original plane of acquisition plus two additional reconstructed planes (Figure 1).



Figure 1. Multipanar display of a fetal heart volume dataset acquired with STIC. Panel 1 shows the original axial acquisition plane showing the 4-chamber view. Panel 2 shows the orthogonal sagittal reconstructed plane. Panel 3 shows the orthogonal coronal reconstructed plane. The green cross represents the intersection between the 3 spatial planes and, in this example, is positioned within the left atrium (LA), adjacent to the posterior wall of the aorta (Ao).

A reference dot or cross is usually used to indicate the point of intersection between the three planes. This reference dot can be moved on the screen with the aid of a mouse, allowing the same structure to be simultaneously visualized in three orthogonal planes. This technology makes possible virtual navigation through a volume dataset (Figure 2).

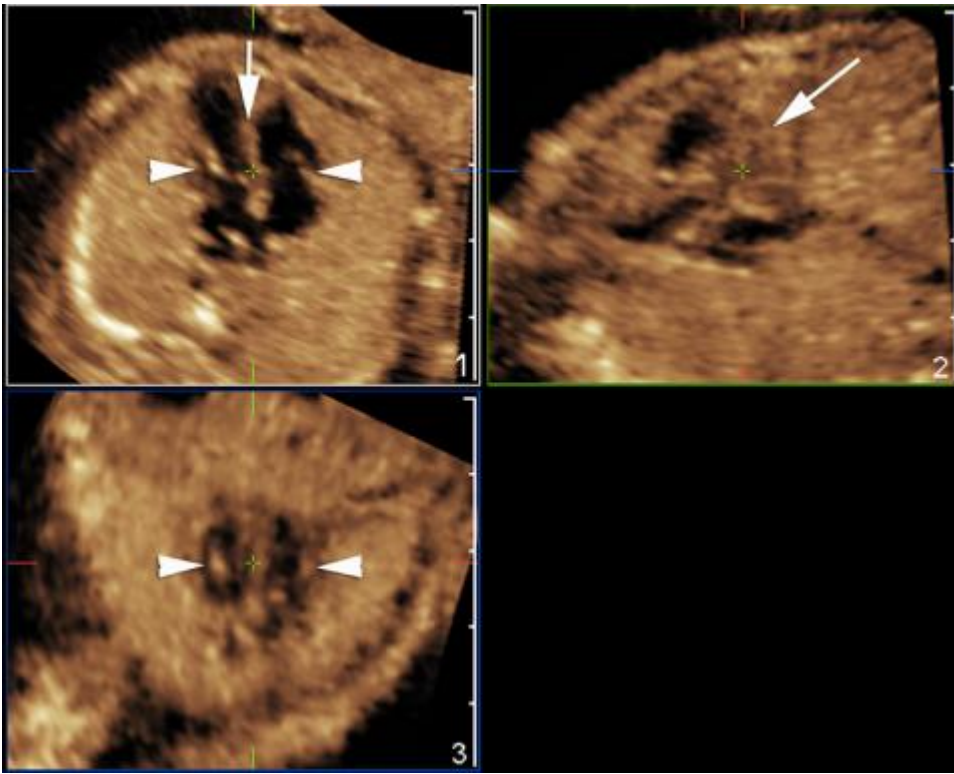


Figure 2. Multiplanar display of a fetal cardiac volume dataset acquired through a transverse section of the fetal chest (same volume shown in Figure 1). The heart is rotated clockwise around the y-axis in Panel 1 until the ventricular septum (arrow) is oriented vertically (apical 4-chamber view). The green cross represents the intersection of the three spatial orthogonal planes. In this case, it is positioned at the crux of the heart. The ventricular septum is seen “en face” on panel 2 (arrow). The annuli of the atrioventricular valves are seen “en face” on panel 3 (arrowheads on panels 1 and 3).

A few techniques have been previously described that may aid the examiner in performing a more purposeful navigation of the volume dataset. One such technique has been called “spin technique”<sup>10</sup> It consists in rotating the volume dataset around the y- or x-axes using the reference dot as a pivot point. The structure being interrogated “opens up” and nicely displays the relationships with other surrounding structures. Another commonly used technique, which was specifically developed to simultaneously display the left and right outflow tracts is known as the “three-step technique”.<sup>4,11</sup> It consists of: 1) re-orienting the fetus on the screen such as that the spine is down; 2) anchoring the reference dot in the middle of the ventricular septum (step 1, Figure 3A); 3) rotating the volume dataset around the y-axis until the continuity between the anterior wall of the aorta and the ventricular septum are seen (step 2, Figure 3B); and 4) moving the reference dot to the level of the aortic valve so that the short axis view of the right ventricular outflow tract is seen simultaneously on the sagittal orthogonal plane (step 3, Figure 3C).

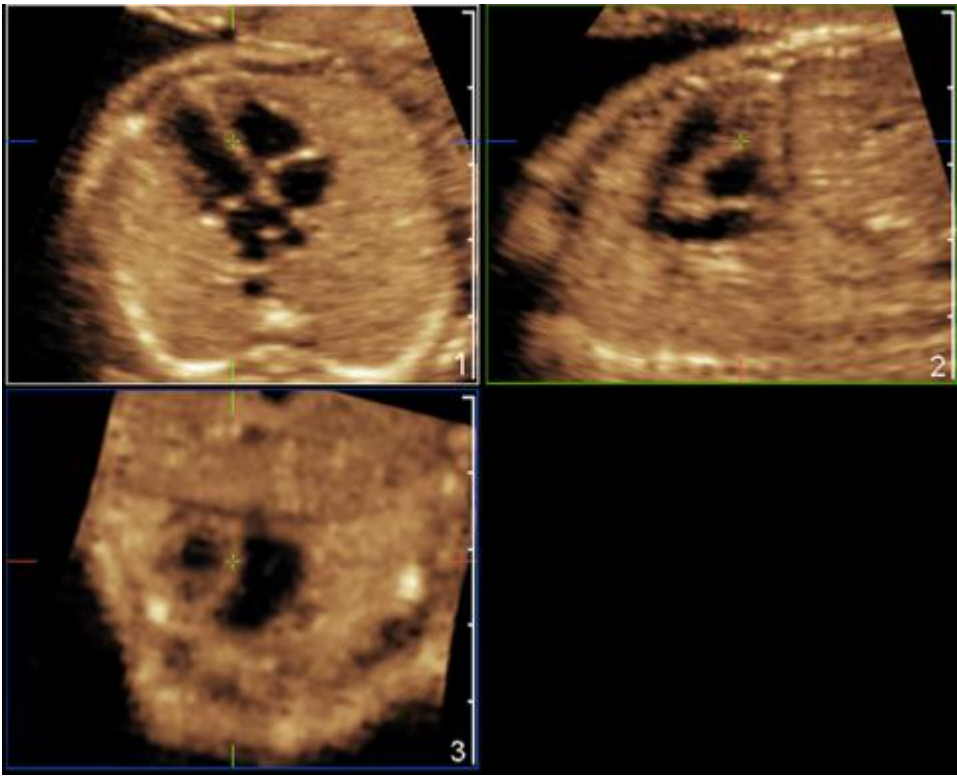


Figure 3a. Three step technique for simultaneous visualization of the left ventricular and right ventricular outflow tracts. 3A) Step 1: 4-chamber view with the fetal spine down; the cross hair is anchored in the middle of the ventricular septum (panel 1).

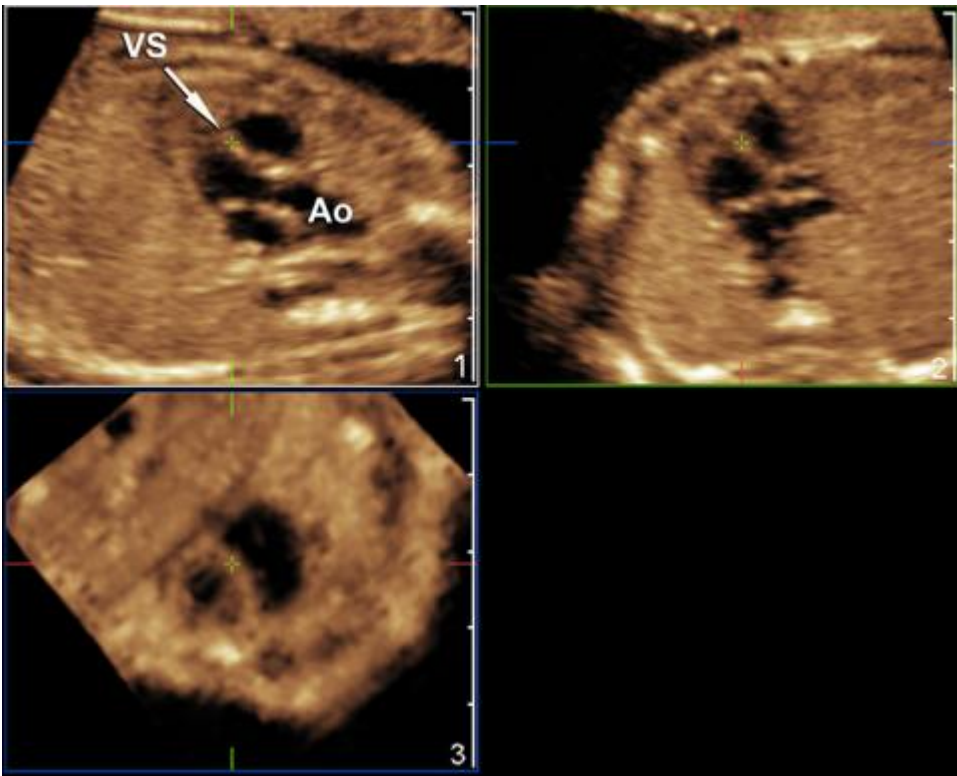


Figure 3b. 3B) Step 2: Rotation of the volume dataset around the y-axis “opens-up” the ventricular septum (VS), showing its normal continuity with the anterior wall of the aorta. In the same image, the reader can see that the posterior wall of the aorta continues with the anterior leaflet of the mitral valve. The long axis view of the left ventricular outflow tract (LVOT) is seen (panel 1).



The long axis view of the left ventricular outflow tract (LVOT) is seen (panel 1). Step 3: the cross hair is moved to the region of the aortic valve (Ao, panel 1) and the short axis view of the right ventricular outflow tract (RVOT) can be seen on the reconstructed sagittal plane (panel 2).

### MULTIFRAME DISPLAY

This method automatically slices the volume dataset in any plane chosen by the examiner.<sup>12,13</sup> Slices are displayed in sequence on the screen. One of the frames (usually the first frame or a side frame) is used as a “scout view” depicting the exact position of the slices within the volume dataset (Figure 4).

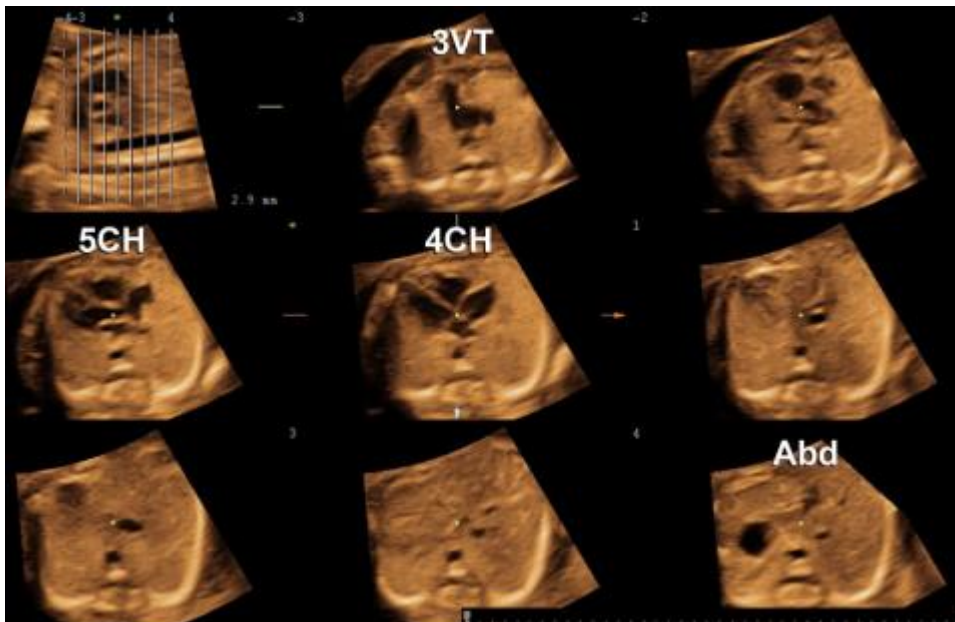


Figure 4. Tomographic ultrasound imaging (multiframe) of a normal fetal heart. The left upper corner image represents the “scout view”. Each vertical line represents that exact position where the slices shown in the remaining 8 frames were obtained. 3VT = 3 vessel and trachea view; 5CH = five chamber view; 4CH = four chamber view; Abd = upper abdomen.

### RENDERING

Rendering is a technology that permits realistic display of 3D volume datasets on a 2D screen (Figures 5

and 6). This is the same technology used to display 3D video games on a flat screen. The examiner can control how the image is displayed and can choose seeing just the surface of the object (surface mode), display the brightest echoes (maximum intensity projection), display the darkest echoes (minimum intensity projection), or display the average intensity of the echoes along the projection path (x-ray mode).

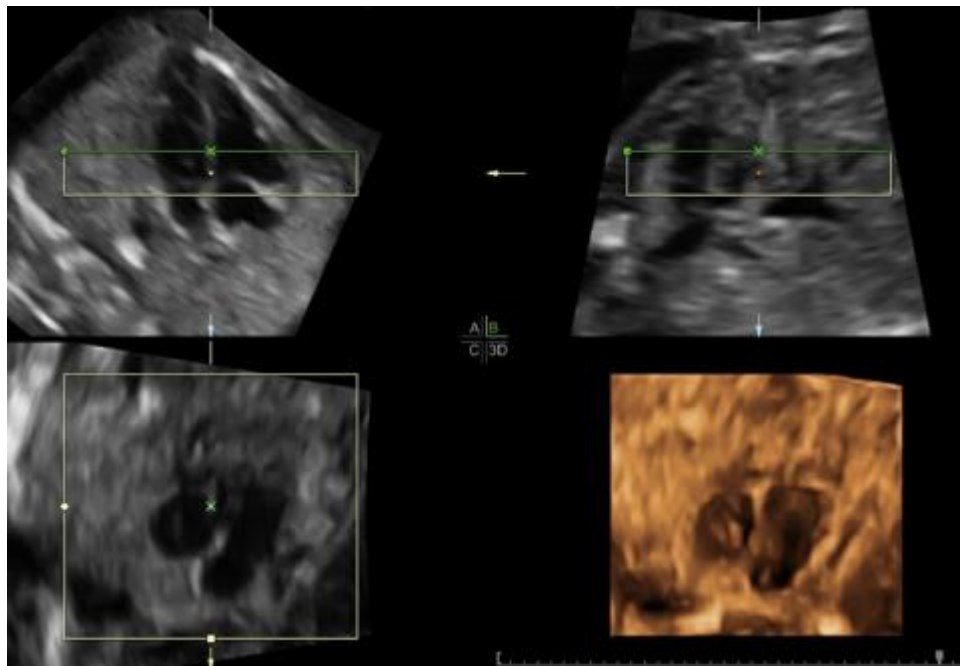


Figure 5. Rendered image of the atrioventricular valves seen “en face” on panel “3D” (right lower quadrant). The image was obtained by placing the region of interest (box) in the region of the atrioventricular valves on panels A and B. The green line indicates direction of view. In this case, it is “top-to-bottom”.

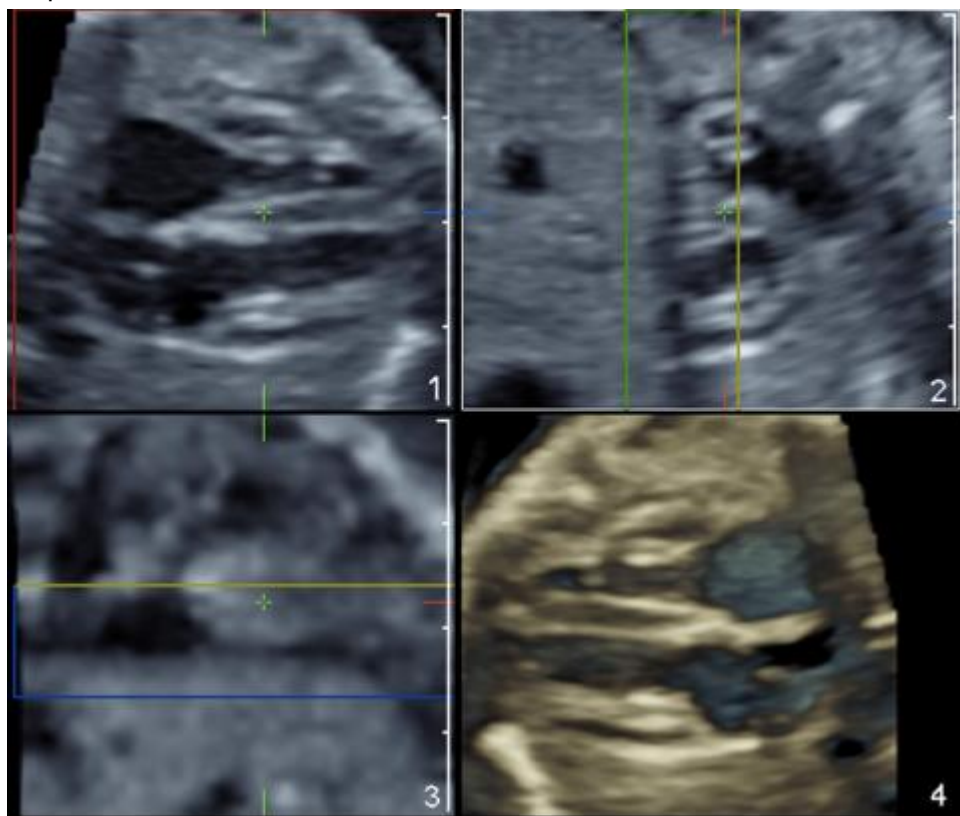


Figure 6. Rendered image of the 4-chamber view seen on panel 4 (right lower quadrant). The region of interest is placed on panel 2, the reconstructed short axis view through the ventricles. The box includes the myocardium and the cardiac base. Direction of view is left-to-right, indicated by the yellow line. Note

the better contrast resolution of the ventricular septum and atrial septum primum on panel 4. The dark oval area underneath the atrial septum seen on panel 4 is the entrance of the IVC.

Rendering using color Doppler, Power Doppler, Inversion Mode and B-Flow Imaging

Any of these modalities can be used to provide “virtual contrast” to the cardiac chambers and blood vessels, so that these structures can be displayed like digital “casts”.<sup>14-22</sup> Figures 7, 8, and 9 provide examples of rendered images of normal fetal hearts using each of these technologies.

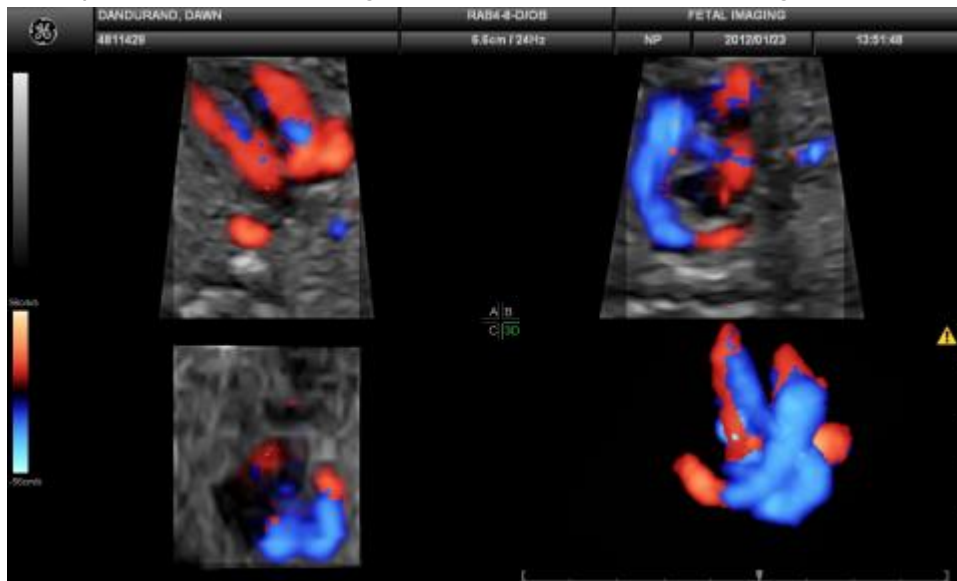


Figure 7. Rendered view of the outflow tracts showing the normal crisscross of the great arteries as they leave the ventricles on panel “3D”. The volume was acquired with color Doppler. RV: right ventricle; LV = left ventricle; Ao = aorta; PA = pulmonary artery.

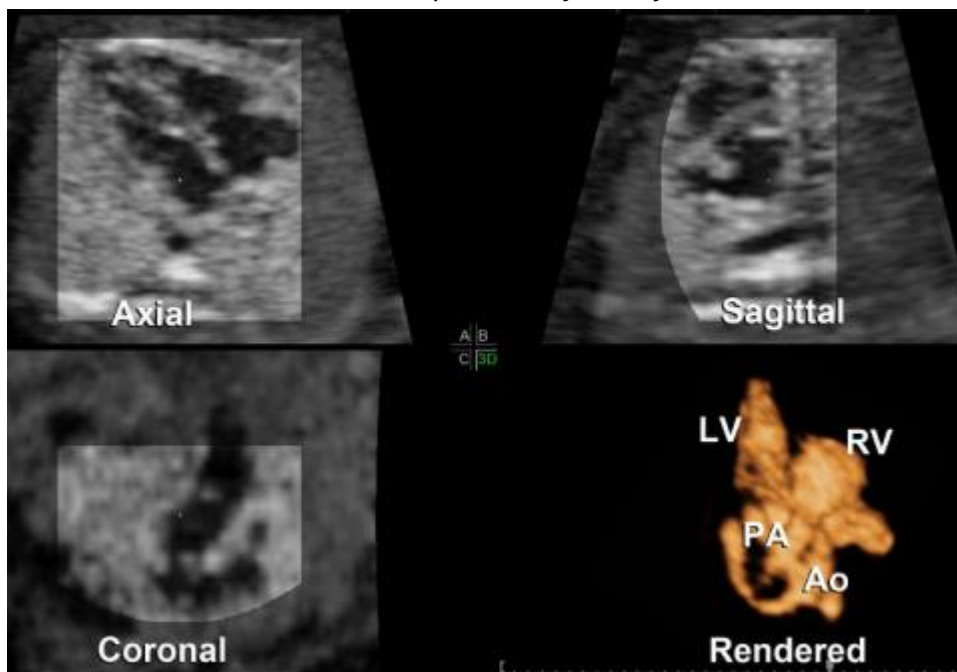


Figure 8. Rendered view of the outflow tracts showing the normal crisscross of the great arteries as they leave the ventricles on panel “3D”. The volume was acquired with gray scale and reconstructed using “inversion” mode. RV: right ventricle; LV = left ventricle; Ao = aorta; PA = pulmonary artery.

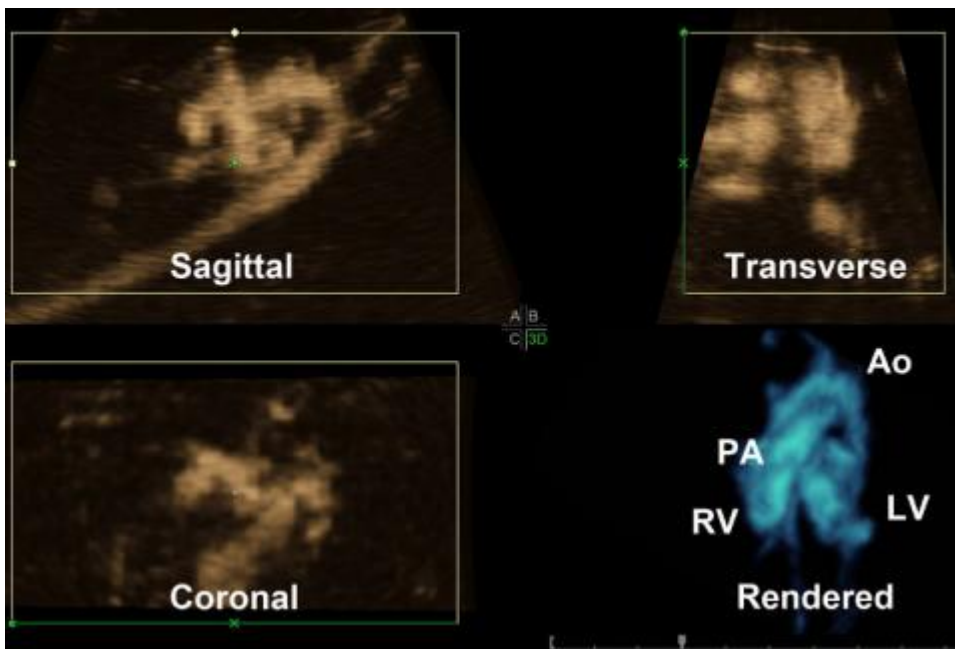


Figure 9. Rendered view of the outflow tracts in a volume dataset obtained with B-flow imaging. The sagittal original plane of acquisition is seen on panel A. The rendered view shows the pulmonary artery (PA) crossing over the aorta (Ao) as it leaves the right ventricle (RV). LV = left ventricle.

## CLINICAL EXAMPLES

The following are clinical examples that illustrate the capabilities of volumetric imaging of the fetal heart.

1. D-Transposition of the great arteries seen using the three-step technique (Figures 10A, 10B, and 10C), and volume rendering with color Doppler (Figure 11)
2. Hypoplastic left heart syndrome due to mitral atresia seen with the Multiframe display (Figures 12A and 12B). From the upper mediastinum to the upper abdomen: 1) retrograde perfusion of the aortic isthmus via a patent ductus arteriosus; 2) normal sized pulmonary artery; 3) small left ventricle with poor/no perfusion.
3. Ebstein anomaly seen with a rendering display, showing the displaced attachment of the septal leaflet of the tricuspid valve to the ventricular septum and the atrialization of the right ventricle (Figure 13).
4. Tricuspid atresia w/ VSD (Figures 14A and 14B). Combined multiplanar and rendered image shows the atretic tricuspid valve and flow to the small right ventricle through a large VSD. There is still forward flow in both the pulmonary artery and aorta with normal crisscrossing demonstrated in Figure 14B.



Figure 10A. Three-step technique demonstrating the classic features of complete transposition of the great arteries (D-TGA). 10A. Normal 4-chamber view on panel A with the reference dot positioned in the mid portion of the ventricular septum. .

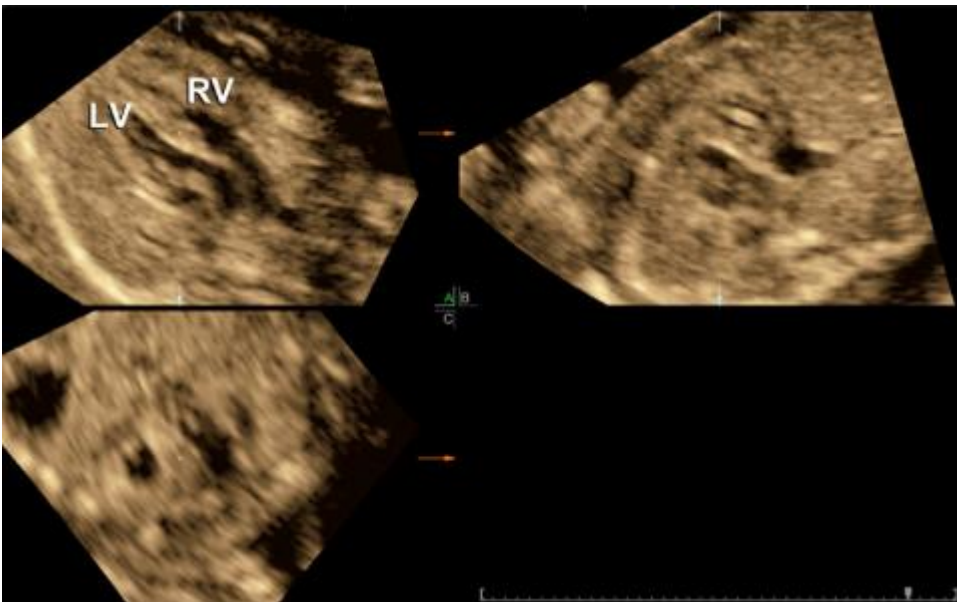


Figure 10B. Three-step technique demonstrating the classic features of complete transposition of the great arteries (D-TGA). 10B. The volume dataset was rotated over the y-axis on panel A until the great vessel leaving the left ventricle is seen. In this case, a parallel vessel leaving the right ventricle is also noted.



Figure 10C. Three-step technique demonstrating the classic features of complete transposition of the great arteries (D-TGA). 10C. The reference dot is moved to the root of the outflow tract leaving the left ventricle, which in this case is the pulmonary artery. The pulmonary artery bifurcation is best seen on panel B. LV = left ventricle; RV = right ventricle; PA = pulmonary artery; Ao = aorta.

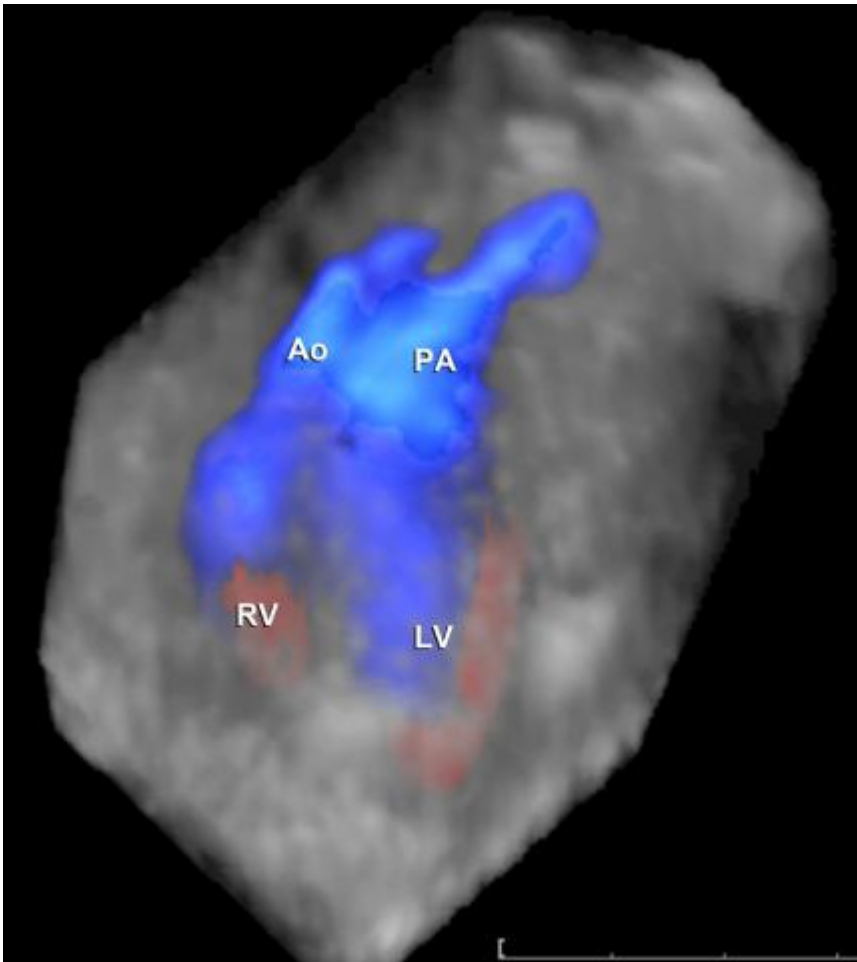


Figure 11. D-Transposition of the great arteries. The aorta (Ao) and main pulmonary artery (PA) arise transposed and in parallel from the right (RV) and left ventricles (LV), respectively.

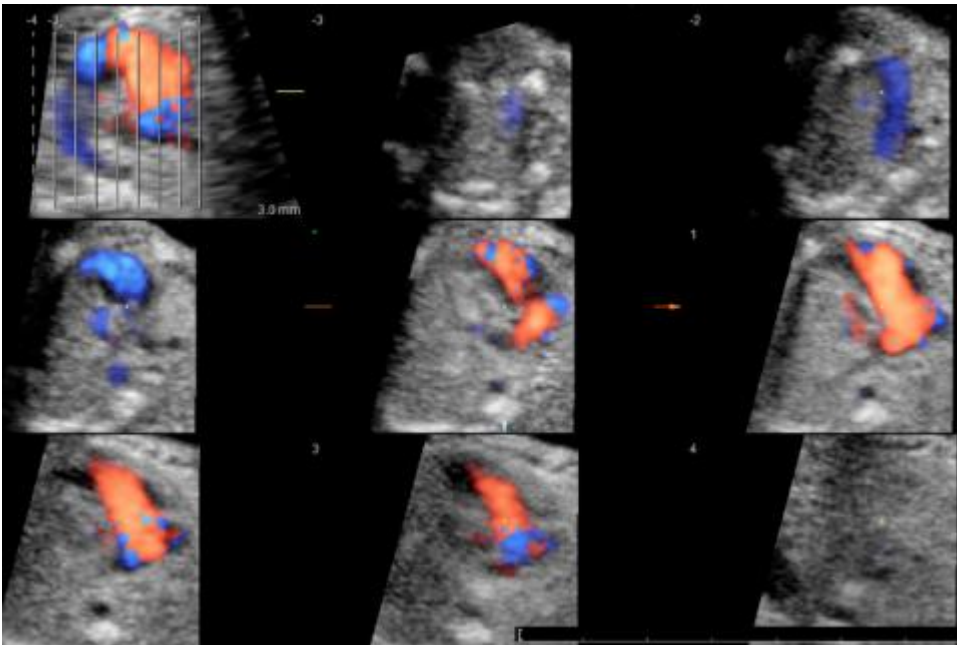


Figure 12A. Hypoplastic left heart syndrome. Multiple axial views of the fetal heart during diastole are shown. At the level of the 4-chamber view (frames 5 through 8), only the right ventricle (RV) is seen filling with blood. The left ventricle (LV) is hypoplastic.

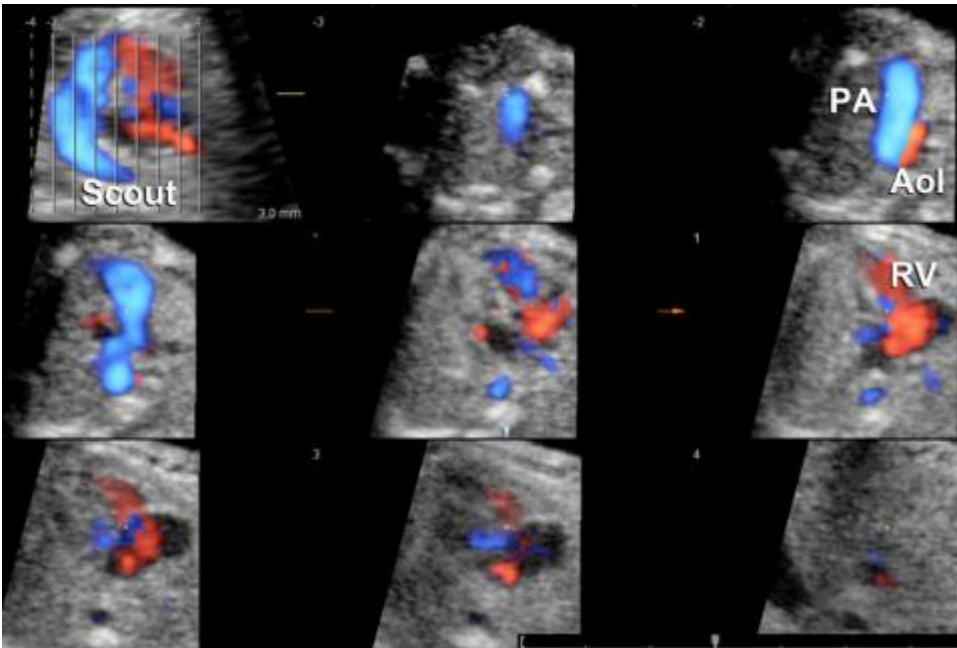


Figure 12B. Multiple axial views of the fetal heart during systole are shown. The pulmonary artery (PA) shows normal forward flow in blue towards the ductus arteriosus (Frame 3). The aorta is not seen; rather, a narrow aortic isthmus (Aol) is shown with retrograde flow depicted by the red color. The findings are consistent with either an atretic aortic valve or critical aortic stenosis.

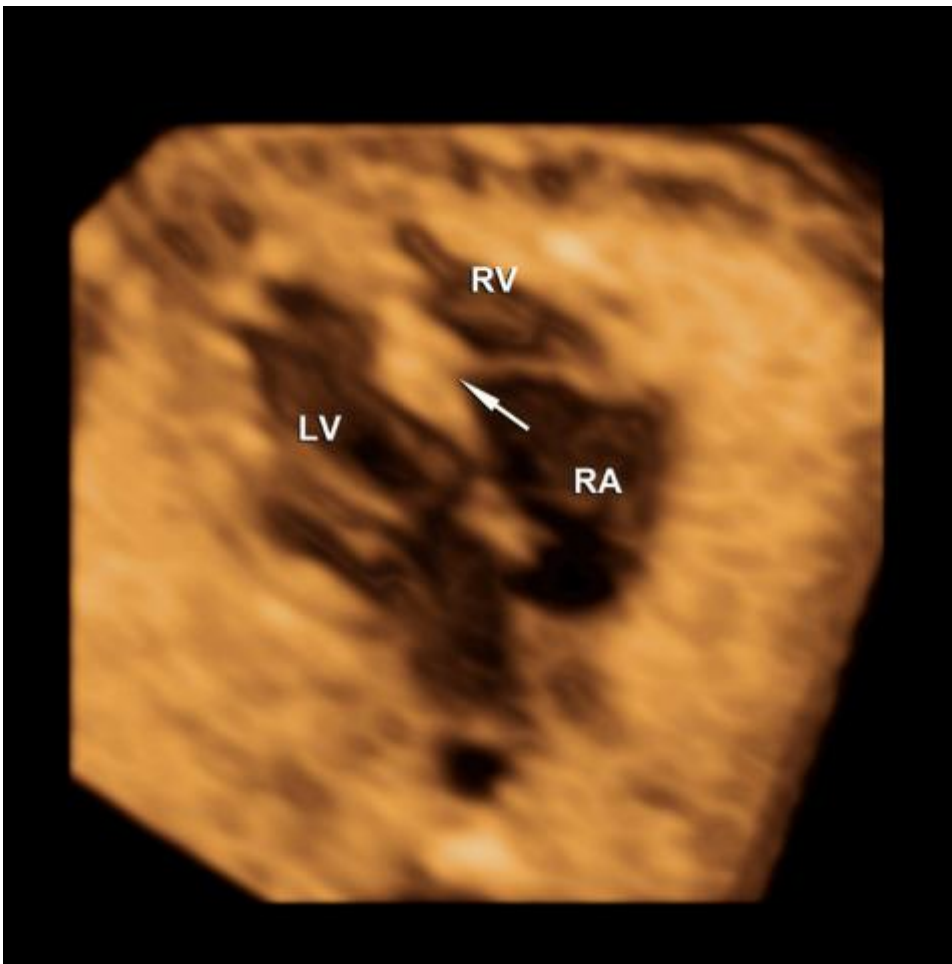


Figure 13. Rendered 4-chamber view of the fetal heart in a fetus with Ebstein's anomaly. The right ventricle (RV) is small and the right atrium (RA) enlarged. The septal leaflet of the tricuspid valve (arrow) is displaced towards the apex.

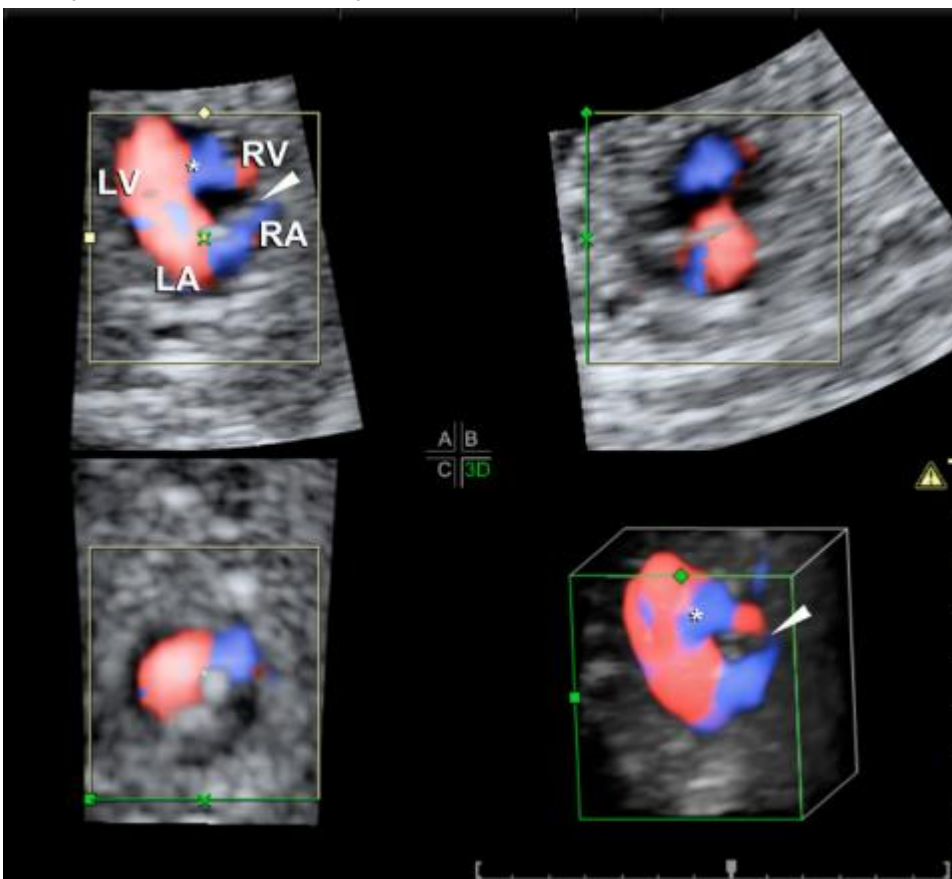


Figure 14A. Tricuspid atresia with VSD shown during diastole. Panel A and the rendered 3D panel shows blood flow from the right (RA) to the left atrium (LA) in blue, then blood flow in red from the LA to the left

ventricle (LV). The hypoplastic right ventricle (RV) is perfused through a large ventricular septal defect (\*). The tricuspid valve (arrowhead) is atretic.

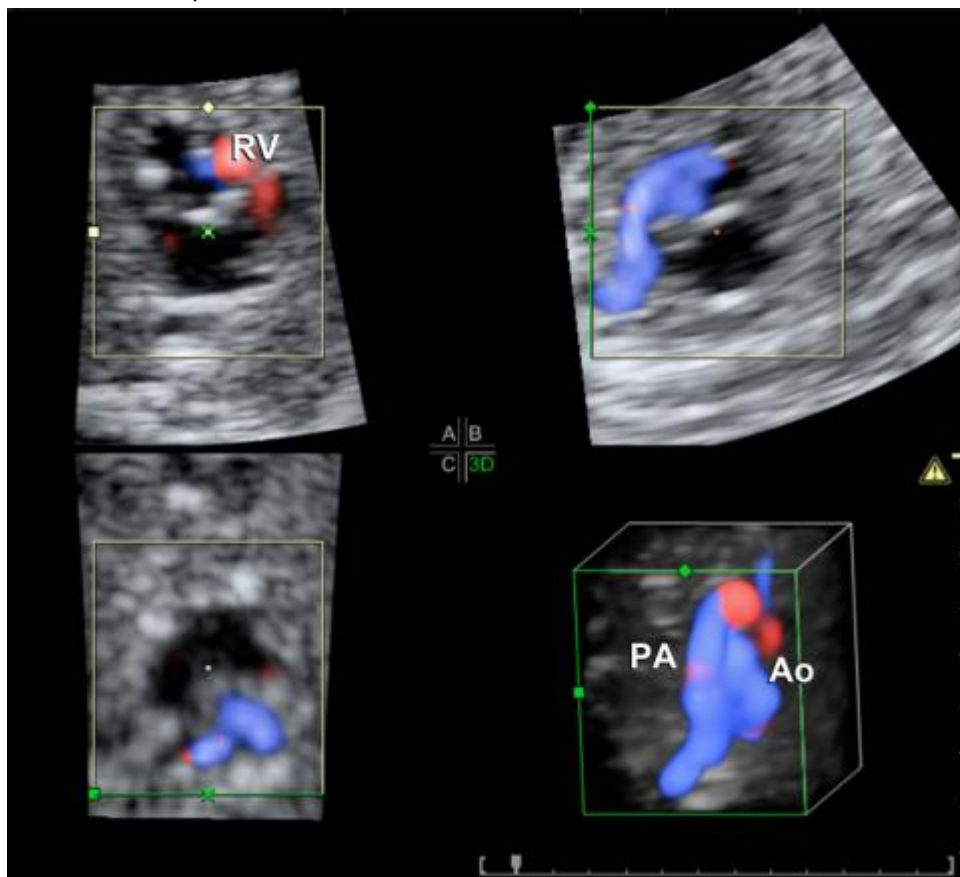


Figure 14B. Despite the hypoplastic RV, the 3D rendered systolic frame depicts forwards blood flow through both the aorta (Ao) and pulmonary artery (PA) during systole.

## FEASIBILITY IN CLINICAL PRACTICE

A few studies have addressed the feasibility or applicability of volumetric imaging of the fetal heart in clinical practice. Uittenbogaard et al.<sup>23</sup> evaluated volumetric images of the fetal heart obtained from 148 patients seen in the clinical setting. All fetuses were high risk and were examined by 2 experienced examiners. No more than 4 attempts at obtaining volume datasets were allowed during each exam. Successful acquisition was possible in 76% of the cases. Twenty-five percent of those were considered high quality, 40% of sufficient diagnostic quality, and 35% were non-diagnostic. Factors associated with high quality volume datasets included a lower body mass index (23.8 kg/m<sup>2</sup> vs. 26.5 kg/m<sup>2</sup>, p=0.04) and posterior placentas (56.0% vs. 30.3%, p=0.05). Visualization rate for cardiac structures was higher for high quality datasets when compared to those of only sufficient diagnostic quality. In a similar study, Cohen et al.<sup>24</sup> determined how frequently satisfactory images for fetal screening could be obtained in nonobese patients scanned at 18 to 22 weeks of gestation, within a maximum examination allotted time of 45 minutes. Satisfactory images of the 4-chamber view, left ventricular outflow tract (LVOT) and right ventricular outflow tract (RVOT) were obtained from the volume datasets by two experienced examiners in 91 to 96.4%, 77.5 to 85.6%, and 80.2 to 87.4% of the time, respectively. A lower frequency of satisfactory images was noted for fetuses with the spine anteriorly positioned, and also when the placenta was anterior.

## TELEMEDICINE APPLICATIONS AND ACCURACY FOR THE DIAGNOSIS OF CONGENITAL HEART

## DISEASE

Volumetric imaging appeals to those interested in telemedicine applications.<sup>25-28, 5</sup> The basic concept is that, particularly in areas with a lack of expertise in fetal echocardiography, volume datasets of the fetal heart could be acquired at the point of care by ultrasound services providers and transmitted to centers with expertise for either a second opinion or definitive diagnosis. Viñals et al.<sup>28</sup> provided instructions to 2 remote examiners by email on how to properly acquire STIC volume datasets of the fetal heart, which were subsequently uploaded to a web server. The volumes were reviewed by a sonologist with experience in fetal echocardiography. All 47 normal fetuses were correctly identified as normal and the 3 fetuses with cardiac defects [ventricular septal defect (VSD), D-transposition of the great arteries (D-TGA), and atrioventricular septal defect (AVSD)] were correctly detected.

More recently, a multicenter international study evaluated the accuracy of remote interpretation of volume datasets collected at several institutions and interpreted by experts who were blinded for the exam indications and outcome. Ninety volume datasets of normal fetuses and fetuses with congenital heart disease were reviewed by experts at 7 different institutions. The sensitivity and specificity for diagnosis of congenital heart disease (CHD) were 93% and 96%, with excellent interobserver agreement (Cohen kappa = 0.97).<sup>25</sup>

A direct comparison between 2D and volumetric fetal echocardiography has also been performed. Bennasar et al.<sup>29</sup> obtained volumes of the fetal heart during 2D fetal echocardiography in 342 fetuses with suspected CHD. Volume datasets were analyzed in a blinded fashion 1 year after the exam. There was no difference in the overall accuracy of 2D fetal echocardiography when compared to volumetric imaging (94.2% vs. 91%,  $p > 0.05$ ). There were 9 false-negative diagnoses with volumetric imaging: 8 cases of VSD and 1 case of aortic arch interruption. Two-dimensional fetal echocardiography did not detect 2 VSDs and 1 case of persistent left superior vena cava. False positive diagnoses for volumetric imaging included: 10 cases of VSDs, 4 cases of coarctation of the aorta, 2 cases of persistent left superior vena cava, 1 case of pulmonic stenosis, and 1 case of rhabdomyoma. False-positive diagnoses by 2D fetal echocardiography were: 1 case of VSD, 4 cases of coarctation of the aorta, 1 case of tricuspid dysplasia, and 1 case of ostium primum atrial septal defect. The authors concluded that, in a high-risk population, volumetric imaging of the fetal heart is as accurate as 2D fetal echocardiography.

## PITFALLS AND ARTIFACTS

Most, if not all, of the pitfalls which occur in volumetric imaging of the fetal heart result from problems during acquisition. Motion and unfavorable fetal position are the most common obstacles to high quality volume datasets. Fetal motion, breathing and hiccups are difficult to control and are associated with artifacts that are best seen on the B-panel of a multiplanar display.

Obtaining good quality volume datasets requires being alert to good opportunities. These present when the fetus is in ideal position (with the spine down), no limbs in front of the chest, and holding still. Sometimes, high quality volume datasets can be obtained from a lateral approach. If the spine is up, excessive shadowing prevents high quality volume datasets to be acquired. Again, there is no way to control the fetus and the best approach is to be prepared when the opportunity presents. This is accomplished by performing the entire examination using volumetric probes. Once the fetus is not moving and the acoustic window to the fetal heart is ideal, the examiner should acquire as many volumes as possible in sequence. These can always be reviewed later and chances are that at least one or two of them will be either diagnostic or of high quality.

Maternal abdominal wall motion due to breathing can be another source of artifact, often times difficult

to control. In this situation, we commonly ask the mothers to take shallower breaths during acquisition or to stop breathing momentarily.

## SUMMARY

Volumetric imaging of the fetal heart is now moving from the highly specialized research laboratories into mainstream clinical practice. This article reviewed the fundamentals of the technology, including volume dataset acquisition and display. Illustrative examples of common congenital cardiac disease were presented to illustrate the potential of the technology. Studies pertaining to the applicability of volumetric imaging of the fetal heart to clinical practice were reviewed, collectively showing that experts can diagnose congenital heart disease with a high degree of accuracy by relying on the volume datasets, suggesting that the technology can be used not only as a problem solving tool, but also as a means to provide access to expert examiners through telemedicine applications

## REFERENCES

1. Deng J. Terminology of three-dimensional and four-dimensional ultrasound imaging of the fetal heart and other moving body parts. *Ultrasound in obstetrics & gynecology : the official journal of the International Society of Ultrasound in Obstetrics and Gynecology* 2003;22:336-44.
2. Nelson TR, Pretorius DH, Sklansky M, Hagen-Ansert S. Three-dimensional echocardiographic evaluation of fetal heart anatomy and function: acquisition, analysis, and display. *Journal of ultrasound in medicine : official journal of the American Institute of Ultrasound in Medicine* 1996;15:1-9 quiz 11-2.
3. DeVore GR, Falkensammer P, Sklansky MS, Platt LD. Spatio-temporal image correlation (STIC): new technology for evaluation of the fetal heart. *Ultrasound in obstetrics & gynecology : the official journal of the International Society of Ultrasound in Obstetrics and Gynecology* 2003;22:380-7.
4. Goncalves LF, Lee W, Chaiworapongsa T, et al. Four-dimensional ultrasonography of the fetal heart with spatiotemporal image correlation. *American journal of obstetrics and gynecology* 2003;189:1792-802.
5. Vinals F, Poblete P, Giuliano A. Spatio-temporal image correlation (STIC): a new tool for the prenatal screening of congenital heart defects. *Ultrasound in obstetrics & gynecology : the official journal of the International Society of Ultrasound in Obstetrics and Gynecology* 2003;22:388-94.
6. Goncalves LF, Espinoza J, Kusanovic JP, et al. Applications of 2-dimensional matrix array for 3- and 4-dimensional examination of the fetus: a pictorial essay. *Journal of ultrasound in medicine : official journal of the American Institute of Ultrasound in Medicine* 2006;25:745-55.
7. Maulik D, Nanda NC, Singh V, et al. Live three-dimensional echocardiography of the human fetus. *Echocardiography* 2003;20:715-21.
8. Sklansky MS, DeVore GR, Wong PC. Real-time 3-dimensional fetal echocardiography with an instantaneous volume-rendered display: early description and pictorial essay. *Journal of ultrasound in medicine : official journal of the American Institute of Ultrasound in Medicine* 2004;23:283-9.
9. Sklansky MS, Nelson T, Strachan M, Pretorius D. Real-time three-dimensional fetal echocardiography: initial feasibility study. *Journal of ultrasound in medicine : official journal of the American Institute of Ultrasound in Medicine* 1999;18:745-52.
10. DeVore GR, Polanco B, Sklansky MS, Platt LD. The 'spin' technique: a new method for examination of the fetal outflow tracts using three-dimensional ultrasound. *Ultrasound in obstetrics & gynecology : the official journal of the International Society of Ultrasound in Obstetrics and Gynecology* 2004;24:72-82.
11. Rizzo G, Capponi A, Muscatello A, Cavicchioni O, Vendola M, Arduini D. Examination of the fetal heart by four-dimensional ultrasound with spatiotemporal image correlation during routine second-trimester

examination: the 'three-steps technique'. *Fetal diagnosis and therapy* 2008;24:126-31.

12. Devore GR, Polanko B. Tomographic ultrasound imaging of the fetal heart: a new technique for identifying normal and abnormal cardiac anatomy. *Journal of ultrasound in medicine : official journal of the American Institute of Ultrasound in Medicine* 2005;24:1685-96.
13. Goncalves LF, Espinoza J, Romero R, et al. Four-dimensional ultrasonography of the fetal heart using a novel Tomographic Ultrasound Imaging display. *Journal of perinatal medicine* 2006;34:39-55.
14. Chaoui R, Hoffmann J, Heling KS. Three-dimensional (3D) and 4D color Doppler fetal echocardiography using spatio-temporal image correlation (STIC). *Ultrasound in obstetrics & gynecology : the official journal of the International Society of Ultrasound in Obstetrics and Gynecology* 2004;23:535-45.
15. Espinoza J, Romero R, Kusanovic JP, et al. Prenatal diagnosis of coarctation of the aorta with the multiplanar display and B-flow imaging using 4-dimensional sonography. *J Ultrasound Med* 2009;28:1375-8.
16. Goncalves LF, Espinoza J, Lee W, et al. A new approach to fetal echocardiography: digital casts of the fetal cardiac chambers and great vessels for detection of congenital heart disease. *Journal of ultrasound in medicine : official journal of the American Institute of Ultrasound in Medicine* 2005;24:415-24.
17. Goncalves LF, Romero R, Espinoza J, et al. Four-dimensional ultrasonography of the fetal heart using color Doppler spatiotemporal image correlation. *Journal of ultrasound in medicine : official journal of the American Institute of Ultrasound in Medicine* 2004;23:473-81.
18. Hata T, Dai SY, Inubashiri E, et al. Four-dimensional sonography with B-flow imaging and spatiotemporal image correlation for visualization of the fetal heart. *Journal of clinical ultrasound : JCU* 2008;36:204-7.
19. Lee W, Espinoza J, Cutler N, Bronsteen RA, Yeo L, Romero R. The 'starfish' sign: a novel sonographic finding with B-flow imaging and spatiotemporal image correlation in a fetus with total anomalous pulmonary venous return. *Ultrasound in obstetrics & gynecology : the official journal of the International Society of Ultrasound in Obstetrics and Gynecology* 2010;35:124-5.
20. Volpe P, Campobasso G, De Robertis V, et al. Two- and four-dimensional echocardiography with B-flow imaging and spatiotemporal image correlation in prenatal diagnosis of isolated total anomalous pulmonary venous connection. *Ultrasound in obstetrics & gynecology : the official journal of the International Society of Ultrasound in Obstetrics and Gynecology* 2007;30:830-7.
21. Volpe P, Campobasso G, Stanziano A, et al. Novel application of 4D sonography with B-flow imaging and spatio-temporal image correlation (STIC) in the assessment of the anatomy of pulmonary arteries in fetuses with pulmonary atresia and ventricular septal defect. *Ultrasound in obstetrics & gynecology : the official journal of the International Society of Ultrasound in Obstetrics and Gynecology* 2006;28:40-6.
22. Volpe P, Tuo G, De Robertis V, et al. Fetal interrupted aortic arch: 2D-4D echocardiography, associations and outcome. *Ultrasound in obstetrics & gynecology : the official journal of the International Society of Ultrasound in Obstetrics and Gynecology* 2010;35:302-9.
23. Uittenbogaard LB, Haak MC, Spreeuwenberg MD, Van Vugt JM. A systematic analysis of the feasibility of four-dimensional ultrasound imaging using spatiotemporal image correlation in routine fetal echocardiography. *Ultrasound in obstetrics & gynecology : the official journal of the International Society of Ultrasound in Obstetrics and Gynecology* 2008;31:625-32.
24. Cohen L, Mangers K, Grobman WA, Platt LD. Satisfactory visualization rates of standard cardiac views at 18 to 22 weeks' gestation using spatiotemporal image correlation. *Journal of ultrasound in medicine :*

official journal of the American Institute of Ultrasound in Medicine 2009;28:1645-50.

25. Espinoza J, Lee W, Comstock C, et al. Collaborative study on 4-dimensional echocardiography for the diagnosis of fetal heart defects: the COFEHD study. *Journal of ultrasound in medicine : official journal of the American Institute of Ultrasound in Medicine* 2010;29:1573-80.

26. Viñals F. Current experience and prospect of internet consultation in fetal cardiac ultrasound. *Fetal diagnosis and therapy* 2011;30:83-7.

27. Viñals F, Ascenzo R, Naveas R, Huggon I, Giuliano A. Fetal echocardiography at 11 + 0 to 13 + 6 weeks using four-dimensional spatiotemporal image correlation telemedicine via an Internet link: a pilot study. *Ultrasound in obstetrics & gynecology : the official journal of the International Society of Ultrasound in Obstetrics and Gynecology* 2008;31:633-8.

28. Viñals F, Mandujano L, Vargas G, Giuliano A. Prenatal diagnosis of congenital heart disease using four-dimensional spatio-temporal image correlation (STIC) telemedicine via an Internet link: a pilot study. *Ultrasound in obstetrics & gynecology : the official journal of the International Society of Ultrasound in Obstetrics and Gynecology* 2005;25:25-31.

29. Bannasar M, Martinez JM, Gomez O, et al. Accuracy of four-dimensional spatiotemporal image correlation echocardiography in the prenatal diagnosis of congenital heart defects. *Ultrasound in obstetrics & gynecology : the official journal of the International Society of Ultrasound in Obstetrics and Gynecology* 2010;36:458-64.